JOURNAL OF AIRCRAFT
Vol. 31, No. 4, July–Aug. 1994

Problem of Dynamic Stall Simulation Revisited

Lars E. Ericsson*
Mt. View, California 94040

Simulating dynamic stall characteristics in subscale wind-tunnel tests often presents an insolvable problem. At stall the peak velocity on the airfoil is several times larger than the freestream velocity, causing compressibility effects to be unusually large. Consequently, simulation requires testing at the full-scale Mach number and Reynolds number, a capability beyond the means of most test facilities. An additional problem is presented by wall interference in so-called two-dimensional dynamic stall tests. Subscale test results are examined against this background of simulation problems.

Nomenclature

c = reference length, airfoil chord
d = cylinder diameter
f = frequency
L = wing lift, coefficient $C_L = L/(\rho_\infty U_\infty^2/2)S$
l = sectional lift, coefficient $c_l = 1/(\rho_\infty U_\infty^2/2)c$
M_∞ = freestream Mach number
m = sectional pitching moment, coefficient $c_m = m/(\rho_\infty U_\infty^2/2)c^2$
p = roll rate
Re = Reynolds number, $R_c = U_\infty c/\nu_\infty$, $R_d = U_\infty d/\nu_\infty$
R_{eff} = effective Reynolds number
r_N = airfoil nose radius
S = reference area, projected wing area
t = time
U = velocity
x = distance from the leading edge
z = translatory coordinate, Fig. 7
α = angle of attack
α_0 = time-average α value
Δ = amplitude
θ = perturbation in pitch
ν = kinematic viscosity
ξ = dimensionless x coordinate, x/c
ρ_N = dimensionless nose radius, r_N/c
ρ_∞ = air density
ω = angular frequency, $2\pi f$
$\bar{\omega}$ = dimensionless frequency, $\omega c/U_\infty$

Subscripts
LP = local peak
N = nose
W = wall
1, 2 = numbering subscripts
∞ = freestream conditions

Derivative Symbols
$\dot{z}$ = $\partial z/\partial t$

Introduction

IN a recent workshop on high-alpha vehicle dynamics, the results shown in Fig. 1 were presented for the NACA-0012 airfoil.[1] Repeating the old test,[2] using a smaller model, c = 2 instead of 4 ft, had not reproduced the sharp lift peak present in the old results.[2] A suggested possible reason for this was a larger side wall interference for the larger model. If this was correct, our interpretation of the old experimental results,[2] and the associated description of the dynamic stall flow processes,[3] could be incorrect. This provided the incentive to revisit the problem of dynamic stall simulation in subscale tests.[4] In addition to applying the unsteady flow concepts developed in Refs. 3 and 4 to the experimental results in Fig. 1, this article describes for the first time how the moving wall effect on transition lowers the effective Reynolds number for turbulent static stall, with associated changes of the dynamic stall characteristics; in some cases leading to laminar dynamic stall.

Discussion

Past simulation experience will be reviewed in order to determine the true reason for the difference in Fig. 1 between the experimental dynamic stall characteristics for the 2-ft and 4-ft chord models of the NACA-0012 airfoil.

Wall Interference

Figure 1 shows the stall to be of the same type for both chord sizes. The 9% larger c_l below stall for the 4-ft chord compared to the 2-ft chord could have been caused by the expected larger two-dimensional top-and-bottom wall interference, as suggested in Fig. 1. Reducing the measured static and dynamic lift of the 4-ft model by 9% gives the results shown in Fig. 2. In the absence of (any difference in) two-dimensional wall interference the results below stall should be the same for both models. The effects of differences in Reynolds number and in Mach number are expected to be insignificant below stall.

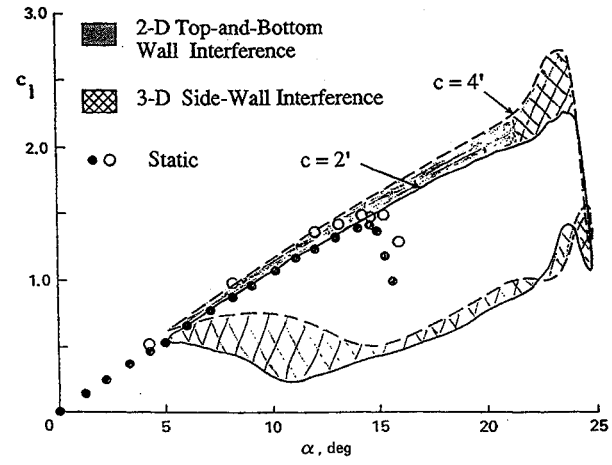

Fig. 1 Effect of model size on dynamic stall characteristics.[1] Oscillating airfoil in a 7- × 10-ft wind tunnel.

Presented as Paper 93-0091 at the AIAA 31st Aerospace Sciences Meeting, Reno, NV, Jan. 11–14, 1993; received Feb. 7, 1993; revision received June 11, 1993; accepted for publication July 26, 1993.

*Engineering Consultant, 1518 Fordham Way. Fellow AIAA.

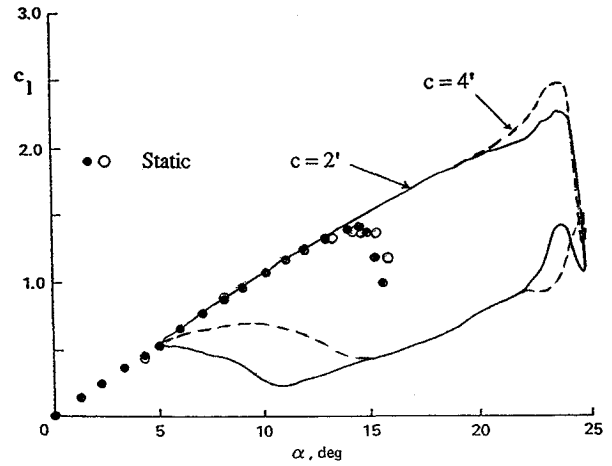

Fig. 2 Effect of model size on dynamic stall characteristics after adjustment for two-dimensional top-and-bottom wall interference.

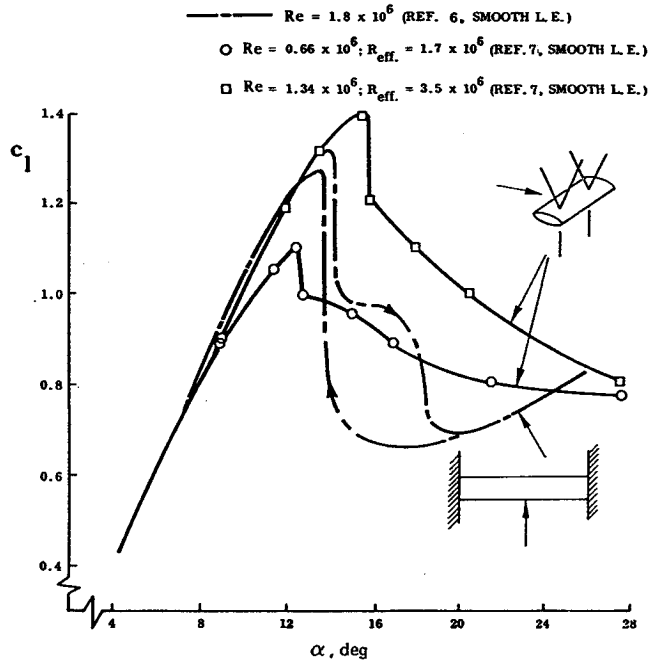

Fig. 3 Effect of side walls on static stall characteristics.

The adjusted dynamic stall results for the 4-ft model shown in Fig. 2 lead to the same description of the dynamic stall phenomenon[3] as the old results[2] shown in Fig. 1. The question that needs to be resolved is whether or not the remaining difference between the dynamic stall overshoot characteristics of the two models could be caused by three-dimensional side wall interference,[5] which is suggested in Fig. 1. The static experimental results for the NACA-0012 airfoil[6,7] shown in Fig. 3 indicate that side wall interference had a negligible influence on the measured $c_l(\alpha)$ characteristics. If the tunnel turbulence levels in the two tests were the same, Fig. 3 would indicate that the side wall interference decreased $c_{l\max}$. This is not unreasonable, as the "tip vortex" generated by the flow separation in the corner, formed by the airfoil and side-wall surfaces[8] (Fig. 4), could not be expected to be as effective as a free tip vortex in venting the leading-edge flow separation on the airfoil.

In any case, Fig. 3 shows clearly that the three-dimensional side wall interference definitely did not increase static $c_{l\max}$, a result in agreement with the static characteristics in Fig. 1, when corrected for two-dimensional wall interference (Fig. 2). Note that the $c_l(\alpha)$ characteristics in Fig. 3 coincide below stall, $\alpha < 8$ deg. As the dynamic c_l peak is generated by the "spilled" leading-edge vortex,[9] it is difficult to see how the

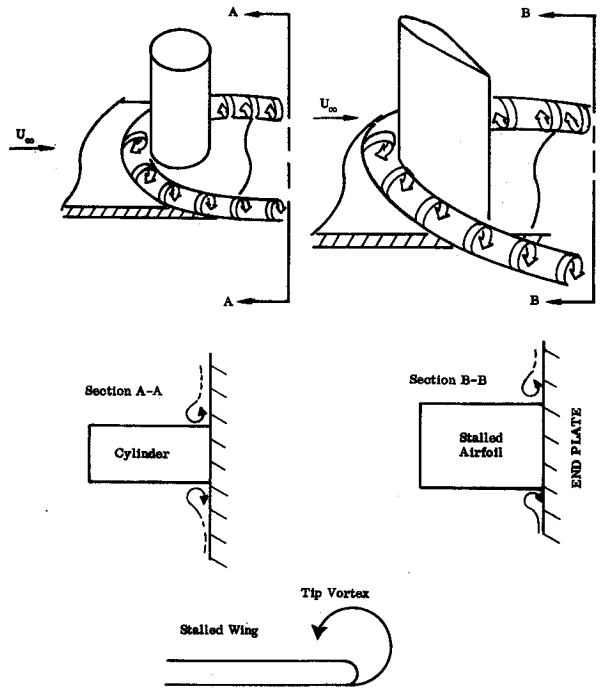

Fig. 4 Side-wall-generated vortex.[8]

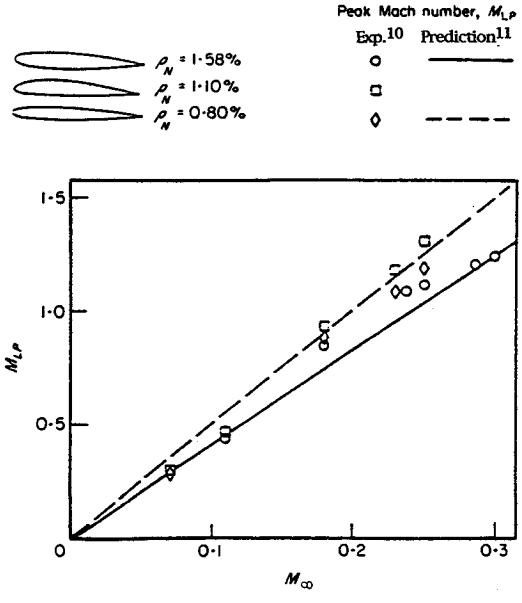

Fig. 5 Peak Mach number on airfoil profiles at α = 15 deg.

side wall interference, if it does anything, could but diminish the generated lift. In the dynamic case, the corner-generated tip vortex does not become free from the airfoil leading edge (Fig. 4), contrary to the case for the tip vortex in the absence of a side wall, when it is free to follow the "spilled" leading-edge vortex[9] in its downstream travel along the airfoil chord. The conclusion to be drawn is the same as earlier in the case of static stall, i.e., side wall interference can not be expected to increase dynamic $c_{l\max}$.

Thus, although side-wall interference is definitely a problem of considerable concern,[4,5] it cannot explain the data trend in Fig. 2. It must have been caused by differences in test Mach number or in Reynolds number.

Compressibility Effects

The test results shown in Figs. 1 and 2 were obtained in a nonpressurized test section. Consequently, when changing the

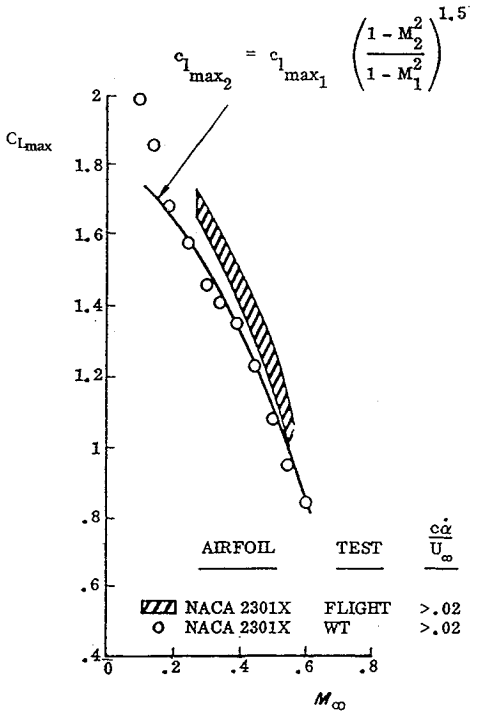

Fig. 6 Effect of freestream Mach number on maximum lift.

model size only one of the two scaling parameters, Reynolds number and Mach number, could remain the same. Considering the fact that the local peak Mach number M_{LP} at stall can be almost an order of magnitude larger than the freestream Mach number, as is illustrated in Fig. 5 by experimental data[10] and prediction,[11] incompressible dynamic stall has little practical application. For example, Fig. 5 shows that even for $M_\infty = 0.1$ the peak Mach number exceeds the "incompressible" limit $M_{LP} = 0.4$. It is shown in Ref. 12 that the dimensionless nose radius $\rho_N = r_N/c$ is the correct scaling parameter for the static lift maximum. It is also shown that increasing the subsonic Mach number will produce an apparent decrease of the effective nose radius, $\rho_N \sim (1 - M_\infty^2)$,[1.5] resulting in a rapid decrease of the static and dynamic lift maximum[13,14] (Fig. 6). In order to keep the Reynolds number the same in the two tests, the test Mach number would have had to be roughly twice as high for the smaller model as for the larger one, resulting in a data trend in agreement with that shown by the experimental results in Fig. 2.

Reynolds Number Effects

The alternative to introducing different compressibility effects is to keep the Mach number the same and conduct the tests at different Reynolds numbers. Judging by past experience,[4,15] this will result in significantly different dynamic stall characteristics. The question is whether the difference would be of the type shown in Fig. 2. It is described in Ref. 4 how the different damping-in-plunge measured at low[16,17] and high[18] Reynolds numbers can be explained by the moving wall effects on the boundary layer (Fig. 7), effects very similar to those measured on a rotating circular cylinder.[19] Figure 7 illustrates how the plunging and pitching airfoils will have opposite moving wall effects during the plunging downstroke $\dot{z}/U_\infty$ and the pitching upstroke θ, in both cases for increasing effective angle of attack.

These moving wall effects on transition were used in Ref. 15 to explain the anomalous subscale test results obtained by Carta.[20] Like Rainey[17] earlier, Carta failed to measure the negative damping in plunge that Liiva[18] observed in his tests, performed at an order of magnitude higher Reynolds number. Not only did Rainey and Carta fail to measure the negative damping expected at full scale Reynolds numbers, the measured damping was actually 50–100% higher in the stall region

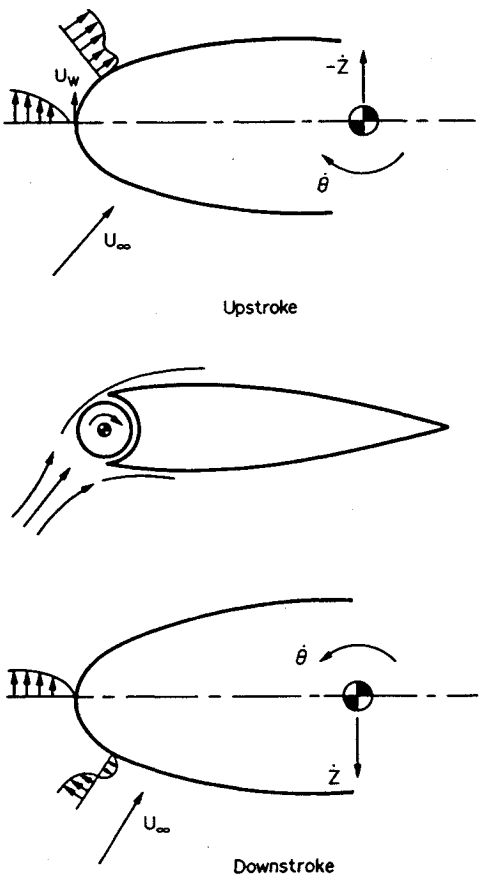

Fig. 7 Leading-edge-jet effect on an airfoil describing pitching or plunging oscillations.[3]

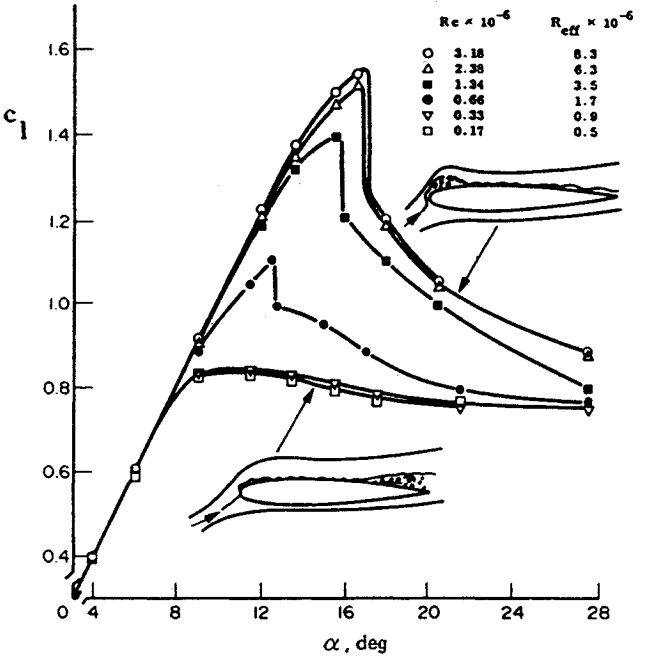

Fig. 8 Effect of Reynolds number on $c_l(\alpha)$ of a NACA-0012 airfoil.[7]

than in the attached flow region. Instead of catching the discontinuous lift loss occurring at higher Reynolds numbers, as in Liiva's test, e.g., $Re = 0.66 \times 10^6$ for the experimental results[7] in Fig. 8, in Carta's and Rainey's tests the moving wall effect on the plunging downstroke had an effect equivalent to increasing the Reynolds number, elevating the lift from, e.g., that for $Re = 0.33 \times 10^6$ to that for $Re = 0.66$ or 1.34×10^6. This caused the area enclosed by the plunging loop to be larger than for attached flow, resulting in the higher

measured damping. The Reynolds number R_{eff} in Fig. 8 attempts to account for the effect of wind-tunnel turbulence.

Thus, the applicability of the moving wall effects measured on a rotating circular cylinder at initially laminar flow conditions to airfoil test results at similar flow conditions is well documented. Consequently, one expects that the moving wall effects on a rotating circular cylinder at initially turbulent flow conditions[19] (Fig. 9) can also be applied to an airfoil at similar ambient flow conditions. In the supercritical flow case, positive Magnus lift is generated at $U_W/U_\infty < 0.1$ (Fig. 9). Magnus lift reversal occurs when the critical U_W/U_∞ – Reynolds number combination is exceeded, causing boundary-layer transition on the top side to be delayed enough to occur in the separated flow region. As a consequence, the flow separation on the top side changes from the supercritical towards the subcritical type. The associated loss of suction lift results in the observed Magnus lift reversal, e.g., for $U_W/U_\infty > 0.1$ at $R_d = 0.42 \times 10^6$. For the pitching airfoil (Fig. 7), accelerated flow and moving wall effects act together[3] rather than opposing each other, as in the case of the plunging oscillations. The result is a very powerful influence on boundary-layer transition, as has been demonstrated for a pitching NACA-0012 airfoil[21] (Fig. 10).

From the above discussion, one can see how the pitch-rate-induced moving wall effect during the upstroke will decrease the effective Reynolds number, e.g., corresponding to going from the $c_l(\alpha)$ characteristics for $Re = 1.34 \times 10^6$ to those for $Re \leq 0.66 \times 10^6$ in Fig. 8. This is exactly the type of data trend exhibited by the experimental results in Fig. 2 when going from the 4-ft to the 2-ft wing chord. This would be expected to occur if the test conditions for the larger model were well above the critical range, e.g., at $Re \geq 2.38 \times 10^6$ in Fig. 8, in which case a lowering of the effective Reynolds number would cause a relatively insignificant decrease of $c_{l\max}$. If the test Reynolds number for the 2-ft chord model had been lower than $Re = 1.3 \times 10^6$, dynamic laminar stall could have occurred, as in the case of the Magnus lift reversal in Fig. 9. This would result in a change of lift characteristics similar to going from $Re = 0.66 \times 10^6$ to $Re = 0.33 \times 10^6$ in Fig. 8. Note that in Fig. 8 the Reynolds number is based upon the airfoil chord, whereas it is based upon the cylinder diameter in Fig. 9.

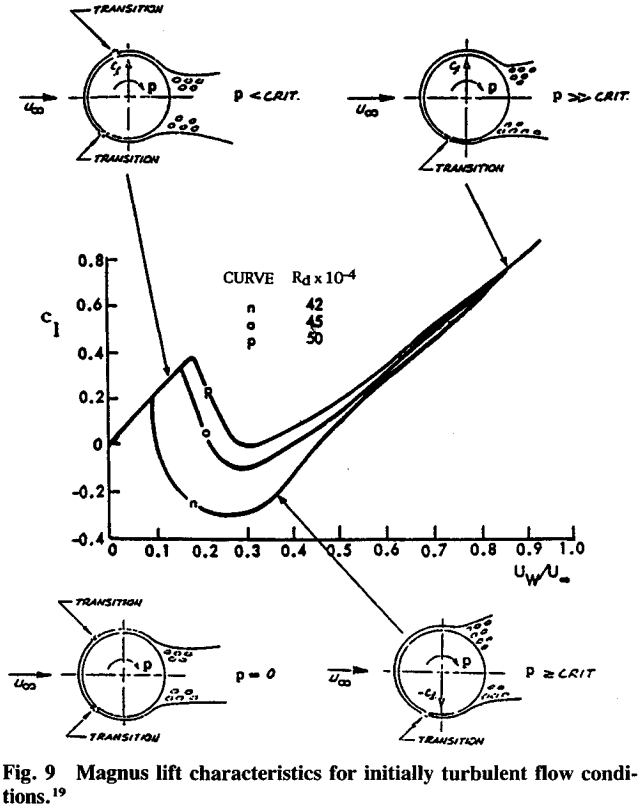

Fig. 9 Magnus lift characteristics for initially turbulent flow conditions.[19]

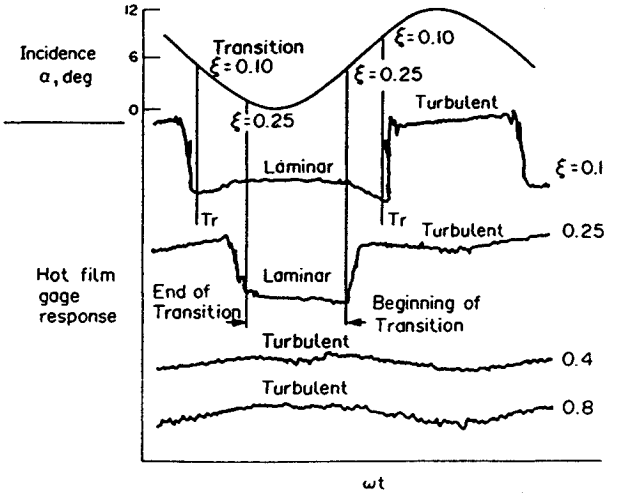

Fig. 10 Hot film response for the NACA-0012 airfoil in pitching oscillation.[21]

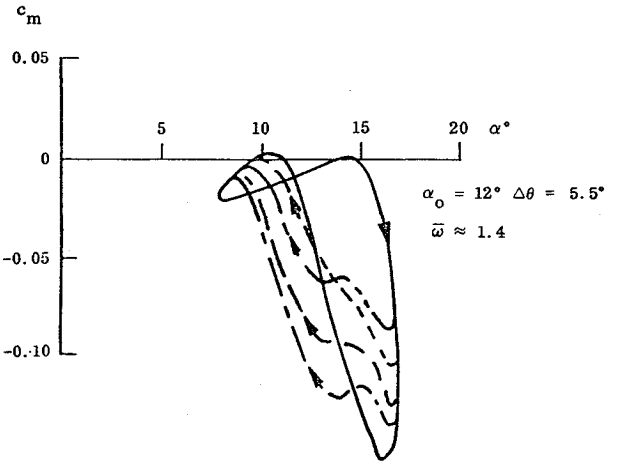

Fig. 11 Nonrepeating consecutive dynamic moment loops.[22]

Thus, the difference in dynamic stall characteristics for the different size models can be explained. What about the different flow reattachment characteristics? Judging by the differences between successive loops for the same airfoil[22] (Fig. 11), the variation of flow reattachment characteristics in Fig. 2 is to be expected even in repeat tests with the same model.

Conclusions

A careful examination of existing information in regard to the problem of dynamic stall simulation reveals that wall interference is not a likely cause of the observed difference in dynamic stall characteristics between the two tests performed with different size models, but rather a lack of the capability to simulate simultaneously both the Mach number and the Reynolds number.

References

[1]McCroskey, W. J., "Two-Dimensional Dynamic Stall—An Experimental Perspective," *Proceedings of AFOSR Workshop on Supermaneuverability: Physics of Unsteady Flows Past Lifting Surfaces at High Angles of Attack*, Lehigh Univ., Bethlehem, PA, 1992, pp. 52–70.

[2]Carr, L. W., McAlister, K. W., and McCroskey, W. J., "Analysis of the Development of Dynamic Stall Based on Oscillating Airfoil Experiments," NACA TN 336, 1977.

[3]Ericsson, L. E., and Reding, J. P., "Fluid Dynamics of Dynamic Stall Part I. Unsteady Flow Concepts," *Journal of Fluids and Struc-*

tures, Vol. 2, 1988, pp. 1–33.

[4]Ericsson, L. E., and Reding, J. P., "Fluid Dynamics of Dynamic Stall Part II. Prediction of Full Scale Characteristics," *Journal of Fluids and Structures*, Vol. 2, 1988, pp. 113–143.

[5]Ericsson, L. E., and Reding, J. P., "Dynamic Stall Simulation Problems," *Journal of Aircraft*, Vol. 8, July 1971, pp. 579–583.

[6]Critzos, C. C., Heyson, H. H., and Boswinkle, R. W., Jr., "Aerodynamic Characteristics of NACA-0012 Airfoil Section at Angles of Attack from 0 to 180°," NACA TN 3361, 1955.

[7]Jacobs, E. N., and Sherman, A., "Airfoil Section Characteristics as Affected by the Reynolds Number," NACA TR 586, 1937.

[8]Ericsson, L. E., and Reding, J. P., "Quasi-Steady and Transient Dynamic Stall Characteristics," Paper 24, AGARD CP-204, Sept. 1976.

[9]Ericsson, L. E., and Reding, J. P., "Dynamic Stall at High Frequency and Large Amplitude," *Journal of Aircraft*, Vol. 17, No. 3, 1980, pp. 140–144.

[10]McCroskey, W. J., McAlister, K. W., Carr, L. W., Pucci, S. L., Lambert, O., and Indergrand, R. F., "Dynamic Stall on Advanced Airfoil Sections," *American Helicopter Society Journal*, Vol. 26, 1981, pp. 40–50.

[11]Ericsson, L. E., and Reding, J. P., "Shock-Induced Dynamic Stall," *Journal of Aircraft*, Vol. 21, No. 5, 1984, pp. 316–321.

[12]Ericsson, L. E., and Reding, J. P., "Stall Flutter Analysis," *Journal of Aircraft*, Vol. 10, No. 1, 1973, pp. 5–13.

[13]Harper, P. W., and Flanigan, R. E., "Investigation of the Variation of Maximum Lift for a Pitching Airplane Model and Comparison with Flight Results," NACA TN 1734, 1948.

[14]Harper, P. W., and Flanigan, R. E., "The Effect of Rate of Change of Angle of Attack on the Maximum Lift of a Small Model," NACA TN 2061, 1949.

[15]Ericsson, L. E., "Effects of Transition on Wind Tunnel Simulation of Vehicle Dynamics," *Progress in Aerospace Sciences*, Vol. 27, 1990, pp. 121–144.

[16]Carta, F. O., "An Analysis of the Stall Flutter Instability of Helicopter Rotor Blades," *American Helicopter Society Journal*, Vol. 12, Oct. 1967, pp. 1–18.

[17]Rainey, A. G., "Measurements of Aerodynamic Forces for Various Mean Angles of Attack on an Airfoil Oscillating in Bending with Emphasis on Damping in Stall," NACA TR 1305, 1957.

[18]Liiva, J., Davenport, F. J., Gray, L., and Walton, I. C., "Two-Dimensional Tests of Airfoils Oscillating Near Stall," USAAVLABS TR 68-13 A&B, Contract DAAJ 02-67-C-0095, Vol. I & II, VERTOL Div., The Boeing Company, April 1968.

[19]Swanson, W. M., "The Magnus Effect: A Summary of Investigations to Date," *Journal of Basic Engineering*, Vol. 83, 1961, pp. 461–470.

[20]Carta, F. O., "A Comparison of the Pitching and Plunging Response of an Oscillating Airfoil," NASA CR-3172, 1979.

[21]McCroskey, W. J., and Philippe, J. J., "Unsteady Viscous Flow on Oscillating Airfoils," *AIAA Journal*, Vol. 13, No. 1, 1975, pp. 71–79.

[22]Liiva, J., and Davenport, F. J., "Dynamic Stall of Airfoil Sections for High Speed Rotors," *Proceedings 24th Annual National Forum of the American Helicopter Society*, Paper 206, Washington, DC, 1968.